



"HENRI COANDA"  
AIR FORCE ACADEMY  
ROMANIA



"GENERAL M.R. STEFANIK"  
ARMED FORCES ACADEMY  
SLOVAK REPUBLIC

INTERNATIONAL CONFERENCE of SCIENTIFIC PAPER  
AFASES 2013  
Brasov, 23-25 May 2013

## A STUDY ON THE ENHANCED PROPERTIES OF A $ZrO_2/20\%Y_2O_3$ CERAMIC COATING BY THERMAL TREATMENT FOR TURBINE BLADES APPLICATION

CRÎȘMARU Ionuț Vasile\*, BĂSESCU Gică Narcis\*, PAPATOIU BINIUC Carmen\*,  
IVANCU Ionel\*, PINTILEI Geanina Laura\*, MUNTEANU Corneliu\*

\*"Gheorghe Asachi" Technical University of Iasi, Faculty of Mechanical Engineering,  
61-63 Prof. dr. doc. D. Mangeron Blvd, 700050, Iasi, Romania

**Abstract:** *The material subjected to the analyses was chosen from the usually used materials in the manufacturing of turbine blades, which enter in the class of Ni base super alloys materials. The material used for the manufacturing of MIG 21 TUMANSKY R-13 turbine blades is of russian provenience. The thermal barrier (TBC) type coating used for turbine blade deposition consists of two layers. The first layer is relatively thin and named bonding layer and the second one is sprayed over the first and has the role of thermal barrier. The bonding layer is made from a MCrAlY ceramic-metal alloy. The purpose of this layer is to protect the base material from oxidation and corrosion and to increase the adherence of the thermal barrier to the base material. The usually used material in the aeronautics industry as thermal insulator is zirconium oxide stabilized with yttrium oxide. Both layers were deposited on the samples with the 7MB METCO installation from Sulzer Metco. The material used for the thermal barrier deposition is the  $ZrO_2/20\%Y_2O_3$  powder. This paper analyses how the samples behave to heat treatment from the point of view of structural changes. After heat treatment the surfaces were analyzed microstructurally and morphologically by electronic microscopy, and in terms of the phase composition by X-ray diffraction.*

**Keywords:** *heat treatment,  $ZrO_2/20\%Y_2O_3$ , SEM, X-ray diffraction*

### 1. INTRODUCTION

The thermal treatments applied to superficial layers obtained by plasma jet spraying have the purpose to induce structural changes and the removal of defects induced by the spraying process. The usage of thermal treatments follows to acquire better mechanical, chemical and technological properties. [1]

The purpose of this paper is to present the results obtained after the thermal treatments and to define how the performance of the coating would improved or how high temperature could lead to the coatings failure.

The heating of the coating leads to a compression of the ceramic material. The temperature gradients make the outer "fibers" of the ceramic to expand but are constrained by the cooler inner "fibers". [5] This leads to a state of compression in the material which tends to buckle the coating. [2] Therefore thermal fatigue accumulates after some thermal cycles which lead to the compressive failure of the coating. [3] Also this type of compressive stresses can develop on cooling due to thermal expansion mismatch between the ceramic and metallic layer. [5] The normal stress produced by the compression combined with the shear stress at the interface amplifies the coatings failure. [5]

## 2. MATERIALS, METHODS AND INSTRUMENTATION

The protection layers were obtained by successive deposition of the bonding and ceramic top layer by air plasma jet method on a 7MB METCO type installation. The parameters used for the plasma spraying deposition are presented in Table 1.

Table 1: Parameters of deposition

Technological parameters	NiCrAlY	ZrO <sub>2</sub> /20%Y <sub>2</sub> O <sub>3</sub>
Spray distance, (mm)	120	120
Injector	1,8	1,8
Plasma gas intensity, (A)	600	600
Arc voltage (U)	62	65
Speed of rotation (rot/min)	55	55
Argon flow (m <sup>3</sup> /h)	50	40
Layer thickness	39-45 μm	200 μm

The thermal treatment applied to the specimens was done with the electric furnace presented in Fig. 1. The furnace is made of a refractive ceramic tube with a length of 500 mm and a outer diameter of 100 mm. The furnace was heated by three nickeline electrical resistances of 100 Ω each, which are parallel connected.



Fig. 1. The electric furnace installation

The Quanta 200 3D electron microscope was used to perform secondary electron images and EDAX analysis, working in the Low Vacuum module at pressures ranging from 50 to 60 Pa and using the LFD (Large Field Detector) detector. The voltage used to accelerate the electron beam had the value of 30kV and a working distance varied from 12 to 15 mm, Fig.2.



Fig. 2. Quanta 200 3D electron microscope

In order to perform a more complete analysis in terms of structural changes due to thermal shock, the ceramic layer was analyzed before and after the test using X-ray diffraction with the X'Pert PRO MRD installation presented in Fig.3.



Fig. 3. X'Pert PRO MRD X-ray diffraction installation

## 3. EXPERIMENTAL RESULTS

In this paper are presented the thermal treatments applied on coatings obtained by plasma jet spraying. The samples were heated to 1000°C for a period of 5, 10 and 15 hours and cooled in air jet at a pressure of 100 bar. After the first 10 minutes the heating of the furnace had a rate of 20°C at every 10 minutes until it reached 1000°C.

The purpose of the heat treatment was to analyze the sintering effect from the point of view from the point of morphological changes and phase transformations. After the heat treatment the surfaces were analysed by electronic microscopy and to highlight the phase composition by X-ray diffraction.

**3.1. Electron microscopy structural analyses of the deposited coatings subjected to thermal treatment** Fig. 4 shows a SEM image of a deposited coating before thermal treatment. In the image two constructive areas



"HENRI COANDA"  
AIR FORCE ACADEMY  
ROMANIA



"GENERAL M.R. STEFANIK"  
ARMED FORCES ACADEMY  
SLOVAK REPUBLIC

INTERNATIONAL CONFERENCE of SCIENTIFIC PAPER  
AFASES 2013

Brasov, 23-25 May 2013

are revealed, the bond layer made of NiCrAlY metallic powder and thermal barrier layer made of  $ZrO_2/20\%Y_2O_3$  ceramic powder. Between the two layers a transition interface is presented. The metallic layer shows a structure formed of elongated grains. These grains get their shape during the spraying process due to the conversion of the high kinetic energy of the sprayed plasma in energy of variation of the shape. [5]

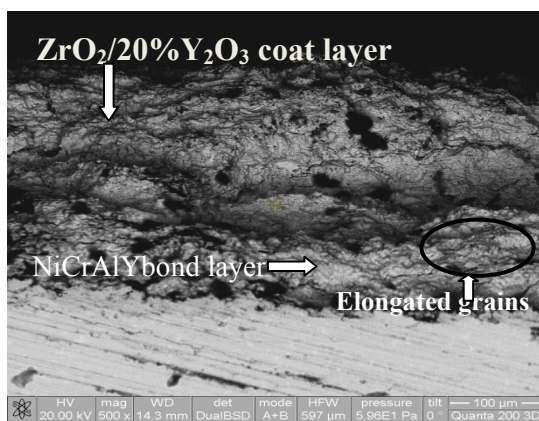


Fig. 4. SEM cross section of the  $ZrO_2/20\%Y_2O_3$  coating layer with the thicknesses  $200\mu m$  without heat treatment

Applying the heat treatment at a temperature of  $1000^\circ C$  for 5 hours led to the increase of the initial pores which resulted in a change of the density value of the material with respect to the analyzed surface (fig. 5). The SEM image also shows the formation of separation surfaces as a result of the oxidation phenomenon.

After the 10 hours heat treatment cracks appeared at the ceramic layer level opened to the outer surfaces. These cracks formed due to the separation of the splats because the weak bond between them (fig. 6). The pores grow even larger with a combine tendency and a more pronounced oxidation phenomenon at the splat limits.

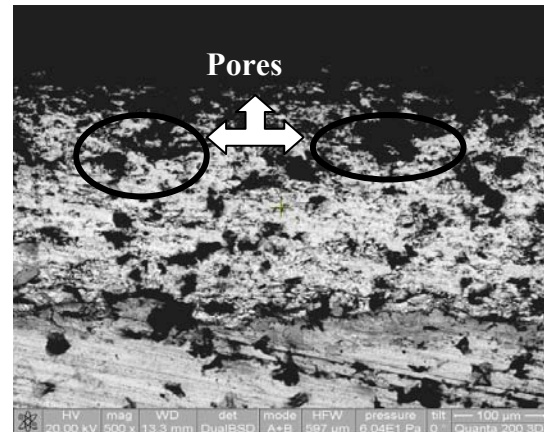


Fig. 5. Microstructure SEM of coated layer in the cross section after the 5 hour heat treatment

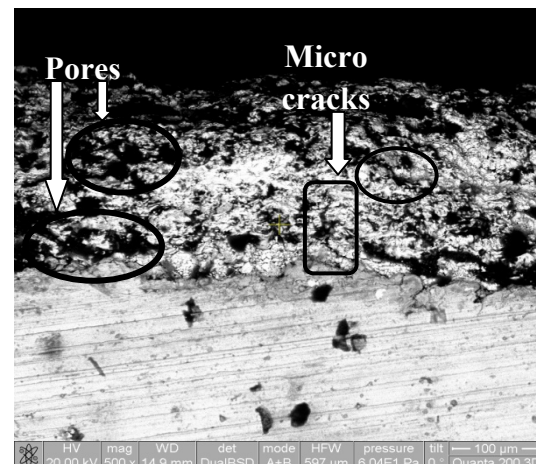


Fig. 6. Cross section of the layer after the 10 hour heat treatment

Increasing the heat treatment duration led to the structural uniformity of the two layers due to the diffusion process. In the SEM image of the coating after the 15 hour heat treatment separation surfaces appeared due to the oxidation phenomenon (fig. 7). The development of these surfaces was differentially produced at the grain limits. The surfaces also tend to show ramifications.



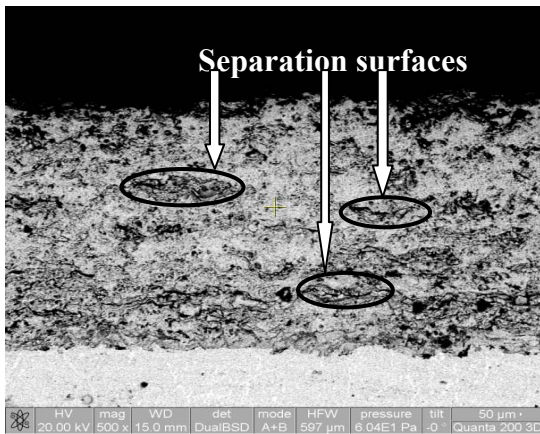


Fig. 7. SEM cross section of the layer after the 15 hours heat treatment

At high magnification, the limits between neighboring splats can be observed with the interlamellar cracks and pores of different dimensions (fig. 8)

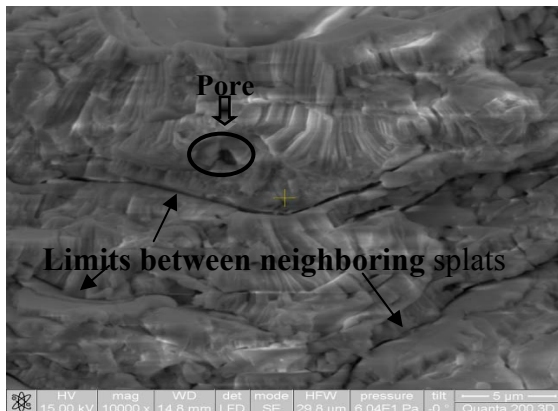


Fig. 8. High magnification cross section of the ceramic layer

After the 5 hour heat treatment at the temperature of 1000°C the splats from the grains tend to divide and the successive disposition of the splats disappears. The structure of the layer is of brick wall type (fig.9).

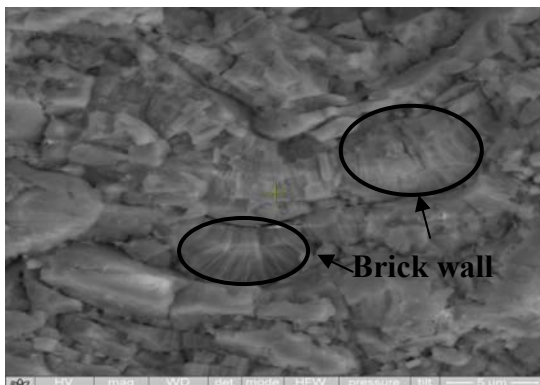


Fig. 9. Cross section of the ceramic layer at high magnification after the 5 hour heat treatment

After the 10 hour heat treatment the separation between the splats is more obvious and the layer prevails with intra splat pores (fig.10).

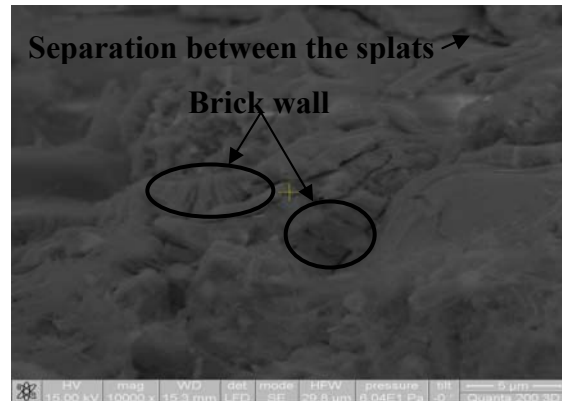


Fig. 10. High magnification of the cross section after the 10 hours heat treatment

After the 15 hour heat treatment at the interface between the ceramic layer and bond layer a sintering of the material was produced (fig. 11). The micro cracks between the splats highlight the brick wall structure of the layer. In individual splats the grains maintained their columnar shape.

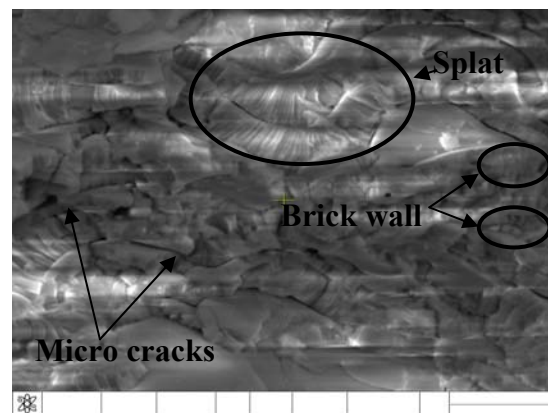


Fig. 11. Cross section of the ceramic layer after heat treatment for 15 hours

**3.2. Structural analyses using X-ray diffraction** The X-ray diffractometer is equipped with a X-ray anode tube made of Cu  $\alpha$ ,  $\lambda = 1.54 \text{ \AA}$ , to which has been applied voltage of 45 kV with a current of 40 A, at an angle of diffraction ( $2\theta$ ) ranging from 25 to 130°. X-ray diffraction analysis was performed in order to observe and highlight the structural changes depending on the number of hours applied to each treatment compared with the phases that were highlighted on the untreated samples (Fig. 12). [1]



"HENRI COANDA"  
AIR FORCE ACADEMY  
ROMANIA



"GENERAL M.R. STEFANIK"  
ARMED FORCES ACADEMY  
SLOVAK REPUBLIC

INTERNATIONAL CONFERENCE of SCIENTIFIC PAPER  
AFASES 2013  
Brasov, 23-25 May 2013

Wavelengths are: K Alpha 1 [ $\text{\AA}$ ]: 1.54060, K-Alpha 2.1,54443, K-Beta [ $\text{\AA}$ ]: 1.39225, K-A2 / K-A1 Ratio: 0.50000.

Structural analysis were performed using a dedicated software (Xpert High Score Plus) through which the crystallographic parameters were identified (lattice type, network constant values a, b and c and angles elementary cell alpha, beta and gamma elementary cell volume, density) and the possible compositional parameters. For the precise choosing of the stoichiometric compositions.

On the cumulative diffractogram was also inserted the specific one for the initial powder. Since the initial powder is a mixture of Zr, Y, O, peaks for all the specific crystallographic planes are present. The XRD patterns of the samples have a smaller number of peaks, on one hand due to the formation of new compounds with new types of crystallographic networks, on the other hand due to the reduced exposure of some crystallographic planes, mainly due to the influence of the substrate and texturing [3].

The determination of the elementary cell parameters is showing the appearance on the substrate of a modified network from the original zirconium oxide. The changes are due to the inclusion in the network of yttrium atoms from the stabilizer.

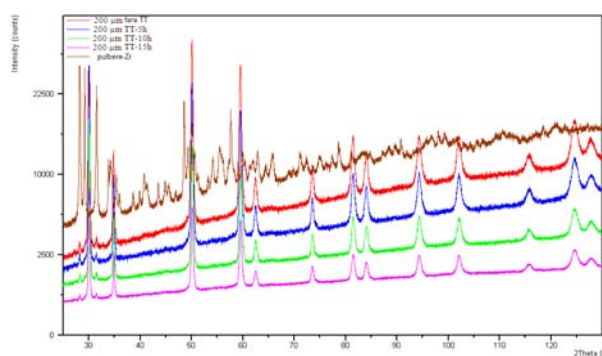


Fig. 12. The X-ray diffractogram for the  $\text{ZrO}_2/20\%\text{Y}_2\text{O}_3$  deposited layer, at an diffraction angle of  $2\theta = 25 \dots 130^\circ$

The zirconium oxide original micro crystalline network maintains after the heat treatment. The network parameters of the original powder are:  $a=5.1240 \text{ \AA}$  and  $c=5.1770 \text{ \AA}$ . After the plasma spraying the network parameters are:  $a=5.1507 \text{ \AA}$ ,  $c=5.3156 \text{ \AA}$  and  $\beta=99.1960^\circ$  (fig. 13). After the heat treatments the network parameters are presented in table 2. It can be observed that the zirconium oxide picks changed from the monoclinic to tetragonal.

Table 2. Parametrii cristalografici

Parametri	Grosimea stratului de 200 $\mu\text{m}$		
	Tratament termic 5 h	Tratament termic 10 h	Tratament termic 15 h
a ( $\text{\AA}$ )	3,6400	3,6120	3,6260
b ( $\text{\AA}$ )	3,6400	3,6120	3,6260
c ( $\text{\AA}$ )	5,2700	5,2120	5,2350
Alfa ( $^\circ$ )	90,0000	90,0000	90,0000
Beta ( $^\circ$ )	90,0000	90,0000	90,0000
Gama ( $^\circ$ )	90,0000	90,0000	90,0000

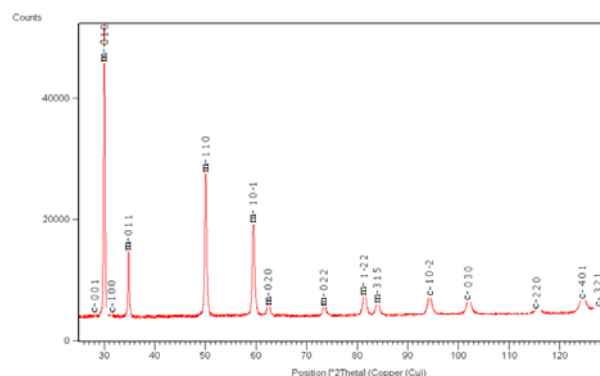


Fig. 13. The X-ray diffractogram of the layer at an diffraction angle of  $2\theta = 25 \dots 130^\circ$

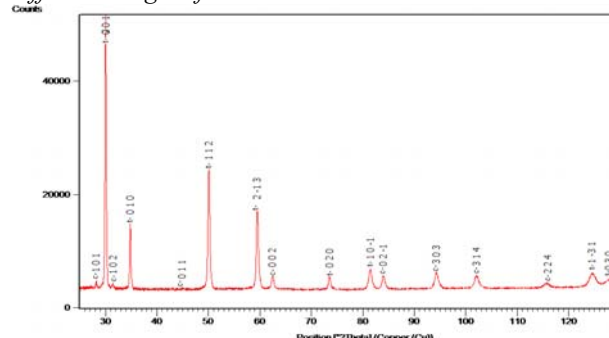


Fig. 14. The X-ray diffractogram after the 5 hours heat treatment, at an diffraction angle of  $2\theta = 25 \dots 130^\circ$

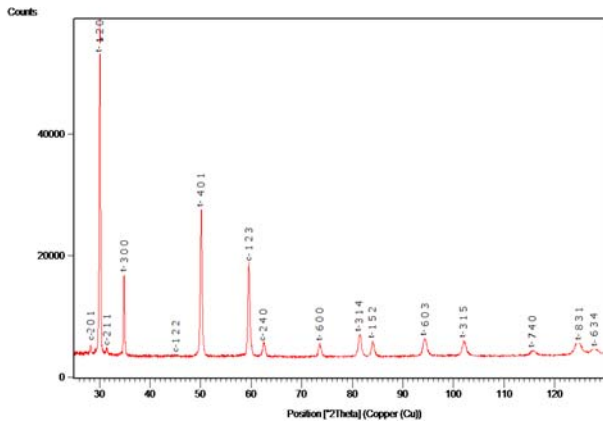


Fig. 15. The X-ray diffractogram after the 10 hours heat treatment, at an diffraction angle of  $2\theta = 25 \dots 130^\circ$

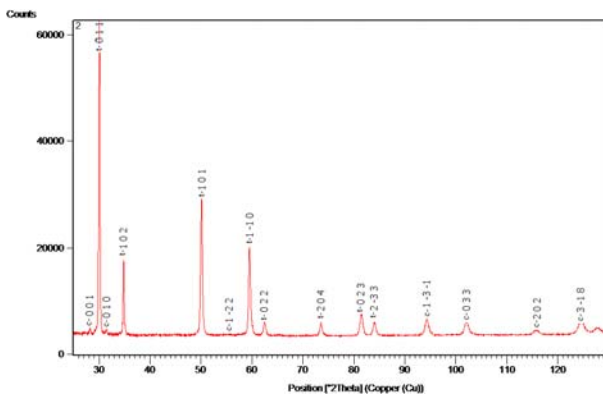


Fig. 16. The X-ray diffractogram after the 15 hours heat treatment, at an diffraction angle of  $2\theta = 25 \dots 130^\circ$

#### 4. CONCLUSIONS & ACKNOWLEDGMENT

After the heat treatment at a temperature of  $1000^\circ\text{C}$  the material matrix becomes more compact. The superficial grains dimension increases due to the forming of bridges between neighboring splats which has a closing effect on the initial micro cracks.

The structure obtained after the thermal deposition have the splats oriented on the direction of the thermal gradient. The heat treatment relaxes the structure and produces an oriented columnar structure of brick wall type. The adherence of the bond layer and thermal layer isn't influenced by the thermal treatment.

After the X-ray diffraction analyses was concluded that by plasma jet deposition the obtained ceramic coating has a multiphase structure. The analyses made after the heat treatment highlighted the changes produced to the multiphase system. The produced grains have a tetragonal structure, stabile at room temperature, which is recommended by the

literature for its good mechanical properties for technological applications.

*Acknowledgment: We thank to SC Plasma Jet SA for the support in the plasma jet deposition of the analysed layer from this paper.*

*I give thanks to the Faculty of Mechanics for the support and for making available the science of materials and Materials Science laboratories for performing the necessary tests for the paper.*

*We thank SC AEROSTAR SA from Bacau for providing the super alloy substrates.*

#### REFERENCES

1. SONG Xiwen, XIE Min, ZHOU Fen, JIA Guixiao, HAO Xihong, AN Shengli, *High-temperature thermal properties of yttria fully stabilized zirconia ceramics*, JOURNAL OF RARE EARTHS, Vol. 29, No. 2, Feb. 2011, p. 155, 2010.
2. Nicholas Curry, Nicolaie Markocsan, Xin-Hai Li, Aure'lien Tricoire, and Mitch Dorfman, *Next Generation Thermal Barrier Coatings for the Gas Turbine Industry*, ASM International, 2010.
3. **Pintilei G.L.**<sup>1</sup>, Brânză F.<sup>2</sup>, Băscescu G.N.<sup>1</sup>, Iacob Strugaru S.C.<sup>1</sup>, Istrate B.<sup>1</sup>, Munteanu C.<sup>1\*</sup>, "The structural transformation of the ceramic layer  $\text{ZrO}_2/20\%\text{Y}_2\text{O}_3$ , obtained by thermal spraying after heat treatment", Universitatea Transilvania din Braşov, 4<sup>th</sup> International Conference "Advanced Composite Materials Engineering" **COMAT 2012-d, 18- 20 October 2012**, Braşov, Romania
4. Chin-Guo Kuo, Hong-Hsin Huang, Cheng-Fu Yang, *Effects of the oxygen pressure on the crystalline orientation and strains of YSZ thin films prepared by E-beam PVD*, Ceramics International 37 (2011) 2037–2041, 2011.2. Harris, M., Johnson, B.J.. Name of the second example paper. *Name of the journal*. Issue (2010).
5. Robert A. Millers and Carl E. Lowell, *Failure mechanisms of thermal barrier coatings exposed to elevated temperatures*, Lewis Research Center, Cleveland, Ohio 44135, NASA (1982)